

## Article

# Reactivation of Frozen Stored Microalgal-Bacterial Granular Sludge under Aeration and Non-Aeration Conditions

Yao Shen <sup>1</sup>, Lin Zhu <sup>1</sup>, Bin Ji <sup>1,\*</sup>, Siqi Fan <sup>1</sup>, Yabin Xiao <sup>1</sup> and Yingqun Ma <sup>2,\*</sup>

<sup>1</sup> Department of Water and Wastewater Engineering, Wuhan University of Science and Technology, Wuhan 430065, China; shy\_13247189423@sina.com (Y.S.); zhuwuster@163.com (L.Z.); a794727614@sina.com (S.F.); xiaoyabing9697@sina.com (Y.X.)

<sup>2</sup> School of Chemical Engineering and Technology, Xi'an Jiaotong University, Xi'an 710049, China

\* Correspondence: binji@wust.edu.cn (B.J.); Yingqun\_Ma@xjtu.edu.cn (Y.M.)

**Abstract:** In this paper, reactivation of microalgal-bacterial granular sludge (MBGS) stored at  $-20\text{ }^{\circ}\text{C}$  for 6 months was investigated under respective aeration (R1) and non-aeration (R2) conditions. Results showed that the granular activity could be fully recovered within 21 days. The average removal efficiency of ammonia was higher in R1 (92.78%), while R2 showed higher average removal efficiencies of organics (84.97%) and phosphorus (85.28%). It was also found that eukaryotic microalgae growth was stimulated under aeration conditions, whereas prokaryotic microalgae growth and extracellular protein secretion were favored under non-aeration conditions. Sequencing results showed that the microbial community underwent subversive evolution, with *Chlorophyta* and *Proteobacteria* being dominant species under both conditions. Consequently, it was reasonable to conclude that the activity and structure of frozen stored MBGS could be recovered under both aeration and non-aeration conditions, of which aeration-free activation was more feasible on account of its energy-saving property. This study provides important information for the storage and transportation of MBGS in wastewater treatment.

**Keywords:** microalgal-bacterial granular sludge; frozen storage; reactivation; wastewater treatment; microbial community



**Citation:** Shen, Y.; Zhu, L.; Ji, B.; Fan, S.; Xiao, Y.; Ma, Y. Reactivation of Frozen Stored Microalgal-Bacterial Granular Sludge under Aeration and Non-Aeration Conditions. *Water* **2021**, *13*, 1974. <https://doi.org/10.3390/w13141974>

Academic Editors: Laura Bulgariu and Antonio Zuerro

Received: 30 May 2021  
Accepted: 16 July 2021  
Published: 19 July 2021

**Publisher's Note:** MDPI stays neutral with regard to jurisdictional claims in published maps and institutional affiliations.



**Copyright:** © 2021 by the authors. Licensee MDPI, Basel, Switzerland. This article is an open access article distributed under the terms and conditions of the Creative Commons Attribution (CC BY) license (<https://creativecommons.org/licenses/by/4.0/>).

## 1. Introduction

Domestic wastewater comes from a wide range of sources and needs to be treated prior to discharge. The conventional activated sludge and aerobic granular sludge (AGS) have been widely applied for domestic wastewater treatment at present, but there are problems such as high energy costs [1], CO<sub>2</sub> emissions [2], large excess sludge production [3,4], etc. In view of this, an innovative and promising microalgal-bacterial granular sludge (MBGS) process has emerged [5]. The advantages of this MBGS process have been illustrated in terms of CO<sub>2</sub> emission reduction, resource recovery, efficiency, and energy-saving in wastewater treatment [6–8]. In addition, the effect of heavy metal and antibiotics on MBGS has been investigated [9,10] in wastewater treatment. Hence, MBGS is gradually becoming an alternative for future wastewater treatment with broad application prospects.

There have been two kinds of MBGS widely reported for wastewater treatment, i.e., aerated MBGS and non-aerated MBGS. The aerated MBGS can be deemed as the development of AGS with illumination [11]. It was reported that aerated MBGS could be applied for low carbon wastewater [12] and saline wastewater treatment [13]. However, similar to the AGS process, the energy cost of aerated MBGS associated with aeration was also concerning. As such, the non-aerated MBGS process has been developed [5,8,14]. Unlike the conventional activated sludge and AGS with the pollutant removal being via both microbial assimilation and dissimilation [15,16], the pollutant removal by non-aerated MBGS mainly relies on microbial assimilation [5] with the synergy between microalgae and bacteria.

Besides environmental factors, e.g., temperature [17] and light [18], the MBGS process may also experience sludge storage and idleness problems, such as sludge transport, inoculation, and process scale-up, which have not been studied so far. Thus, it makes sense to investigate the storage and reactivation of MBGS for practical applications in municipal wastewater treatment. In addition, frozen storage is a common means of granule preservation. For instance, AGS was studied for frozen storage and reactivation [19,20]. As such, it is of significant importance to know whether frozen storage is suitable for MBGS. Moreover, it is also unknown whether the reactivation of MBGS depends on aeration.

Therefore, this study aimed to compare the reactivation of frozen stored MBGS under aeration and non-aeration conditions. The granular characteristics, reactor performance, microbial communities, and possible mechanisms were studied. It is expected that the study would provide some valuable information for MBGS practical applications in regard to its storage and reactivation.

## 2. Materials and Methods

### 2.1. Synthetic Municipal Wastewater

The composition of the synthetic wastewater mainly consisted of about 527.0 mg/L NaAc, 113.1 mg/L  $\text{NH}_4\text{Cl}$ , 50.0 mg/L  $\text{MgSO}_4 \cdot 7\text{H}_2\text{O}$ , 30.3 mg/L  $\text{KH}_2\text{PO}_4$ , 40.0 mg/L  $\text{FeSO}_4 \cdot 7\text{H}_2\text{O}$ , 20.0 mg/L  $\text{CaCl}_2$ , and 40.0 mg/L  $\text{NaHCO}_3$ . The concentrations of organics, phosphorus, and ammonia were about 400.0 mg/L, 5.0 mg/L, and 30.0 mg/L, respectively.

### 2.2. Experimental Setup

The experiments were conducted in two open conical flask reactors (R1 and R2) with the effective volume of 500 mL in this study. MBGS was stored frozen at  $-20\text{ }^\circ\text{C}$  in a fridge for six months without the addition of any chemicals. Two reactors with the above-mentioned synthetic wastewater as feed were exposed to a light-emitting diode (LED) light at a photosynthetic photon flux density (PPFD) of about  $180\text{ }\mu\text{mol}/\text{m}^2/\text{s}$ . R1 was continuously aerated from the bottom at a flow rate of around 4 L/min, while R2 was not aerated. The hydraulic retention time was controlled at 12 h. Typical dissolved oxygen (DO) concentrations were 5–7 mg/L and 4–5 mg/L in R1 and R2 at the end of the cycle, respectively. The frozen stored MBGS was continuously activated under continuous light at a room temperature of around  $25\text{ }^\circ\text{C}$  for 21 days.

### 2.3. Microbial Community Analysis

Sludge samples from the initial stage, aeration, and non-aeration reactors (referred to as R0, R1, and R2, respectively) were collected. DNA extraction, PCR amplification, and sequencing were performed for bacteria and microalgae based on prokaryotic primer 338f-806r [21] and eukaryotic primer 528f-706r [22] targeting 16S rRNA and 18S rRNA, respectively. The samples were biogenetically analyzed using the Illumina MiSeq platform, and the raw sequence data can be obtained from the NCBI under the accession number PRJNA715013.

### 2.4. Analytical Methods

Chemical oxygen demand (COD), ammonia–nitrogen ( $\text{NH}_4^+\text{-N}$ ), phosphate–phosphorus ( $\text{PO}_4^{3-}\text{-P}$ ), mixed liquor suspended solids (MLSS), mixed liquor volatile suspended solids (MLVSS), and 5-min sludge volume index ( $\text{SVI}_5$ ) of the water samples were determined according to standard methods [23]. MLSS and MLVSS were maintained at  $2.4 \pm 0.20\text{ g/L}$  and  $2.2 \pm 0.25\text{ g/L}$ , respectively. The particle size distribution of the activated MBGS was compared using particle size analyzer (Mastersizer 2000, Ver. 5.60, Malvern, UK). The DO concentrations were tested with a YSI 5100 DO meter (Yellow Springs, OH, USA). The extracellular polymeric substance (EPS) was extracted using a modified thermal extraction method [24], which consisted of proteins (PN) and polysaccharide (PS). The PN content was detected using a modified Lowry method, and the PS content was obtained using a phenol–sulfuric acid method [24]. The total chlorophyll (total

Chl) content, including chlorophyll-a (Chl-a) and chlorophyll-b (Chl-b), was extracted using an acetone extraction method [25]. The specific oxygen production rate (SOPR) of MBS was determined using a respiration method [26].

### 2.5. Statistical Analysis

Statistical analysis was performed using IBM SPSS version 22 to analyze the reactor performance of MBS under aeration and non-aeration conditions for significance with  $p < 0.05$  and the Pearson coefficient for correlation analysis.

## 3. Results and Discussion

### 3.1. Reactor Performance

Figure 1 illustrated the influent and effluent concentrations and removal efficiencies of COD,  $\text{NH}_4^+$ -N, and  $\text{PO}_4^{3-}$ -P during the activation of the frozen stored MBS with the aeration (R1) versus the non-aeration reactor (R2). The experimental process was divided into two phases. The first 14 days was the activation phase (Phase I) and the subsequent 7 days was the stable phase (Phase II).

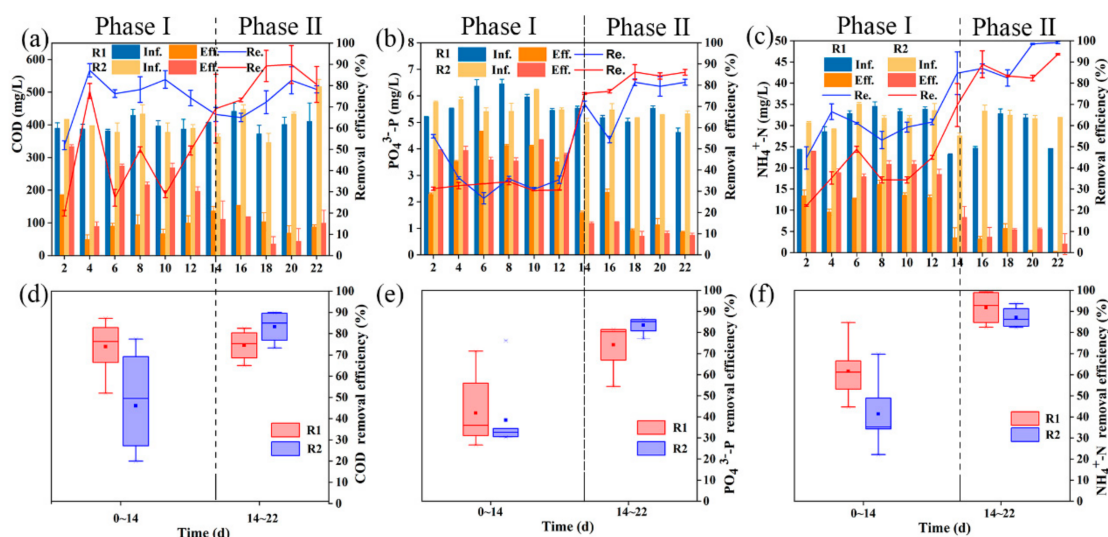


**Figure 1.** Profiles of influent and effluent concentration, removal efficiency: (a) COD; (b)  $\text{PO}_4^{3-}$ -P; (c)  $\text{NH}_4^+$ -N; and boxplot of removal efficiency of two group reactors during the reactivation process: (d) COD; (e)  $\text{PO}_4^{3-}$ -P; (f)  $\text{NH}_4^+$ -N. (R1: Aeration; R2: Non-aeration).

In Phase I, as illustrated in Figure 1d–f, R1 and R2 exhibited respective average removals of COD (76.28%, 49.52%),  $\text{PO}_4^{3-}$ -P (35.93%, 32.68%) and  $\text{NH}_4^+$ -N (61.18%, 35.26%), suggesting that R1 showed superior average removal efficiency, especially for COD and  $\text{NH}_4^+$ -N removal ( $P < 0.05$ ) (Figure 1d,f). In Phase II, as shown in Figure 1d–f, R1 and R2 showed excellent removal efficiencies on average (COD: 75.29%, 84.97%;  $\text{PO}_4^{3-}$ -P: 80.44%, 85.28%;  $\text{NH}_4^+$ -N: 92.78%, 86.23%), which were comparable to previous studies [27,28], indicating that MBS almost had been fully activated. It was also found that  $\text{NH}_4^+$ -N removal was consistently superior in R1, while R2 showed higher removal efficiencies for COD and  $\text{PO}_4^{3-}$ -P. The better  $\text{NH}_4^+$ -N removal of R1 than R2 could be ascribed to that the bacteria growth could be promoted under aeration conditions, and the bacteria ( $\text{C}_5\text{H}_7\text{O}_2\text{N}$ ) could have higher nitrogen content than microalgae ( $\text{C}_5\text{H}_8.9\text{O}_{1.8}\text{N}_{0.6}$ ), as revealed by their empirical formulas [29]. However, the better COD and  $\text{PO}_4^{3-}$ -P removal in R1 than R2 could be ascribed to the higher abundance of heterotrophic bacteria and phosphorus accumulating organisms, respectively. In addition, the removal of COD,  $\text{NH}_4^+$ -N, and  $\text{PO}_4^{3-}$ -P exhibited an increasing trend in both R1 and R2 (Figure 1a–c), reflecting the recovery of MBS under both aeration and non-aeration conditions. It was worth mentioning in Figure 1a that the highest removal efficiencies (82.53% and 89.97%) and the lowest effluent

concentrations (69.37 and 43.75 mg/L) for COD were achieved on day 20 in both R1 and R2. In view of this, the activity of frozen stored MBGS could be fully recovered after about 20 days of activation.

### 3.2. Morphological and Characteristic of MBGS

After being in frozen storage for 6 months, the MBGS became dark and lusterless, which was caused by the long-term anaerobic condition; after 21 days of being fully activated, granules turned green and brownish green in R1 and R2, respectively (Figure S1). The total Chl content of R1 and R2 were 22.28 mg/g-VSS and 5.53 mg/g-VSS, respectively, indicating that the color change of the MBGS was consistent with the variation of total Chl content shown in Figure 2a.

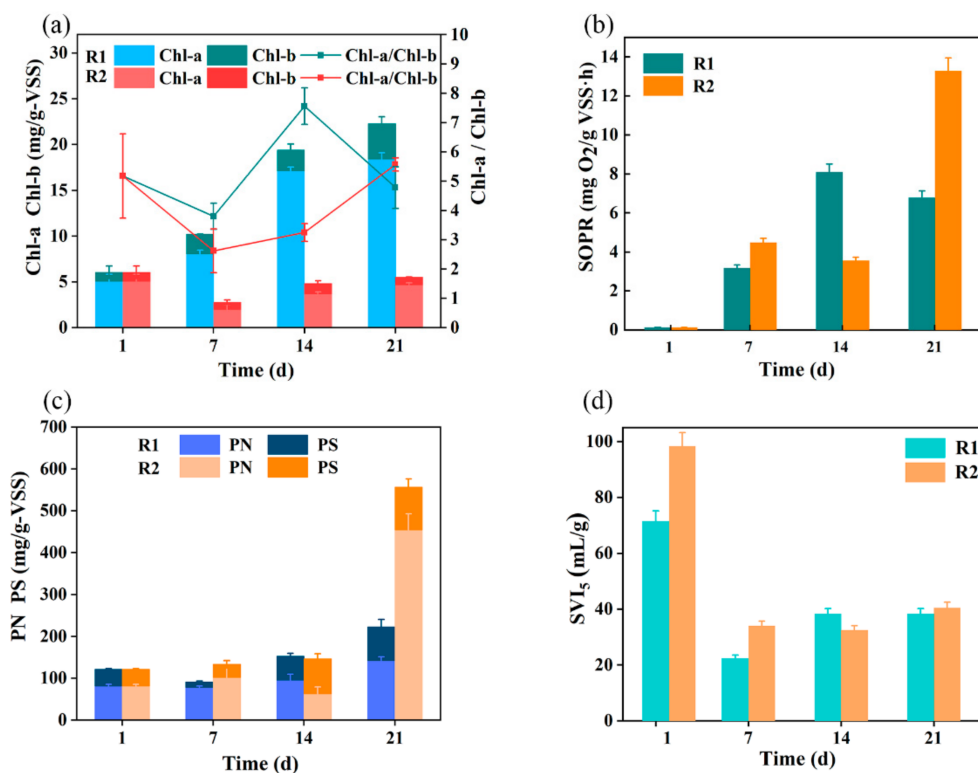


**Figure 2.** Variations in properties of microalgal-bacterial granular sludge during the reactivation process. (a) Chl-a, Chl-b, Chl-a/Chl-b; (b) SOPR; (c) PN, PS; (d) SVI<sub>5</sub>. (R1: Aeration; R2: Non-aeration).

It can be observed from Figure 2a that the Chl-a content increased sharply from the initial 5.07 mg/g-VSS to 18.43 mg/g-VSS in R1 after 21 days of activation, while Chl-b also increased from 0.98 mg/g-VSS to 3.85 mg/g-VSS. However, the content of Chl-a and Chl-b showed slight variation in R2. The sharply increased total Chl content in R1 indicated that the aeration conditions facilitated microalgae growth. Furthermore, the Chl content was related to particle size, which was also influenced by aeration. The small size MBGS due to the shear force generated by aeration in R1 (Figure S3), expanded the specific surface area and improved light utilization efficiency [30,31], resulting in the fast growth of microalgae. In addition, the increase in chlorophyll in Phase I of R1 was a prediction for Phase II, suggesting that the suspended microalgae would grow.

As shown in Figure 2b, the SOPR gradually increased in both reactors. R1 had almost reached a steady state within the first 14 days due to aeration, while R2 showed a sharp increase to 13.28 mg O<sub>2</sub>/g VSS·h on day 21. This indicated that the non-aerated MBGS could generate oxygen after activation. Figure 2c illustrates that the variations of PN, PS, and EPS content in R1 and R2. EPS content did not significantly change during the

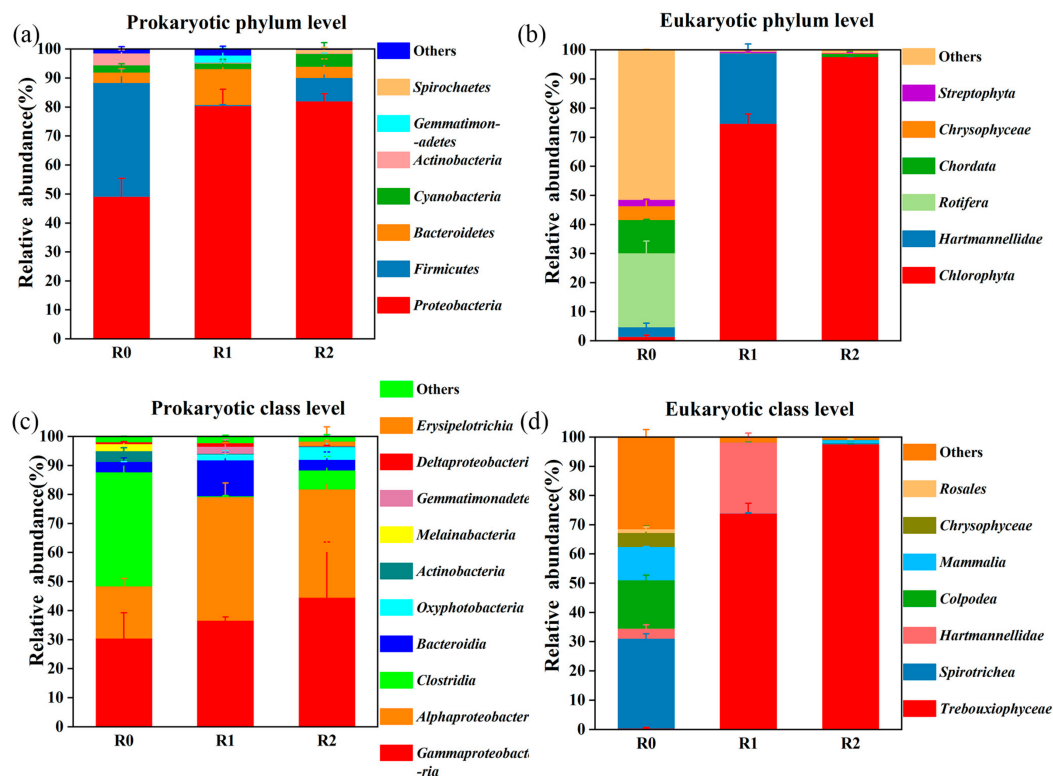
first 14 days, but increased on day 21, especially for R2. Significantly, PN content of R2 drastically increased to 454.45 mg/g VSS, while the PS content remained relatively stable, implying that PN might play a crucial role in MBGS recovery, which was similar to AGS recovery in idle conditions [32].

Figure 2d shows the initial SVI<sub>5</sub> of 71 mL/g and 98 mL/g in R1 and R2 respectively, resulting in relatively poor settle ability. After 21 days of full activation, SVI<sub>5</sub> were stabilized at 38 mL/g and 40 mL/g in R1 and R2, respectively (Figure 2d), with all granules recovering excellent settle ability, which could be reflected by the increased EPS content and microalgae growth [22,33], as indicated in Figure 2a,c.

### 3.3. Microbial Community Succession

The relative abundance variation of prokaryotic communities is shown in Figure 3a,c. The initial, aerated, and non-aerated samples referred to R0, R1, and R2, respectively. At phylum level, R0, R1, and R2 were mainly composed of *Proteobacteria* (49.16%, 80.47%, 82.04%), *Firmicutes* (39.34%, 0.34%, 8.12%), *Actinobacteria* (4.13%, 0.31%, 0.20%), *Bacteroidetes* (3.56%, 12.41%, 3.90%), and *Cyanobacteria* (2.46%, 1.97%, 4.44%). Clearly, *Proteobacteria* was the most abundant species in both R1 and R2. Moreover, previous studies had also elaborated that *Proteobacteria* and green algae were correlated [12], which both increased in this study (Figure 3a,b). Meanwhile, *Firmicutes*, *Actinobacteria* and *Clostridia* decreased substantially (Figure 3a,c). However, more *Clostridia* (39.31%) belonging to phylum *Firmicutes* (39.34%) in R0 indicated the presence of more anaerobic and facultative anaerobic bacteria during the storage period [34,35]. In addition, representatives of *Burkholderiaceae*, *Xanthomonadaceae* and *Sphingomonadaceae* belonging to phylum the *Proteobacteria* were identified. Some of these bacteria were known to contain microcystin-degrading species [36], which may have enabled their growth in the reactor along with the microalgae. However, we did not test for microcystins. As seen in Figure 3c, the prokaryotic community became dominated by members of the classes *Alphaproteobacteria* (42.52%, 37.28%) and *Gammaproteobacteria* (36.71%, 44.60%) in R1 and R2. Notably, the higher abundance class *Gammaproteobacteria* (44.60%) in R2 was favorable for the initiation and maturation of MBGS due to its secretion of EPS [18], which was correlated with the EPS content shown in Figure 2c. Furthermore, part of the increased EPS content might be the result of *Rhodanobacteraceae* and *Xanthomonadaceae* [37].

Distinctive differences in the relative abundance of eukaryotic communities are observed in Figure 3b,d. At the phylum level, R0 consisted mainly of *Chordata* (11.44%) and *Rotifera* (25.42%), but *Chlorophyta* (74.73%, 97.67%) became the dominant phylum in R1 and R2 (Figure 3b). Clearly, the abundance of *Chlorophyta* was higher in the non-aerated MBGS, implying that non-aeration conditions might be more favorable for the growth of *Chlorophyta*. In addition, as shown in Figure 3d, *Trebouxiophyceae* (73.97%, 97.60%) was the most abundant species in R1 and R2 at the class level, but *Spirotrichea* (30.69%) and *Colpoda* (16.55%) of R0 disappeared in R1 and R2 after activation, demonstrating a shift in the photosynthetic composition after the activation eukaryotic microbial community. It should be noted that the eukaryotic microalgae in R1 was more abundant than in R2, as reflected by Figure S3 and the Chl-b content in Figure 2a, while R2 appeared to have a more abundant prokaryotic microalgae, implied by a slightly higher Chl-a to Chl-b ratio [38] in R2 than in R1 (Figure 3a).



**Figure 3.** Microbial community of microalgal-bacterial granular sludge at phylum and class levels (>1% relative abundance). (a) prokaryotic phylum; (b) eukaryotic phylum; (c) prokaryotic class; (d) eukaryotic class. (R0: Initial; R1: Aeration; R2: Non-aeration).

### 3.4. Potential Functional Characteristics of Microorganisms

To further understand the organics and phosphorus removal of MBGS under aeration and non-aeration conditions, potential functional groups were classified at genus level including heterotrophic bacteria (HB) and phosphorus-accumulating organisms (PAO) (Table 1). *Pseudomonas* and *Thauera*, as both HB and PAO [39,40], could favor efficient organics and phosphorus removal, which were found to be much more abundant under non-aeration conditions (R2) than in aeration conditions (R1). A higher abundance of *Aquimonas* and *Acinetobacter* in R2 than R1 might also contribute to organics degradation and phosphorus removal, respectively [34,41]. Overall, the higher abundance of both HB and PAO in R2 than in R1 could be responsible for the better organics and phosphorus removal under non-aeration conditions than in aeration conditions for the recovered MBGS. As for nitrogen removal, the better performance of R1 could be achieved since aeration could promote the growth of bacteria, while increasing the bacteria to microalgae ratio in the MBGS as discussed.

The possible removal pathways of COD, N, and P are shown in Figure 4. It depicts that the reactivation of the frozen stored MBGS could have considerably different pollutant removal pathways under aeration and non-aeration conditions. It suggests that external oxygen could alter the functional characteristics with regard to pollutant removal in the MBGS for wastewater treatment.

**Table 1.** The potential key functional microbial groups at the genus level.

Key Functional Groups		Relative Abundance (%)			Reference
		R0	R1	R2	
Heterotrophic Bacteria	<i>Pseudomonas</i>	0.43	1.36	15.79	[39]
	<i>Thauera</i>	0	0.02	7.01	[40]
	<i>Acinetobacter</i>	12.47	0.32	3.21	[41]
	<i>Flavihumibacter</i>	0.02	11.5	0.02	[42]
	<i>Pseudoxanthomonas</i>	0.04	6.84	1.04	[39]
	<i>Aquimonas</i>	0.01	0.15	7.9	[34]
Phosphorus-Accumulating Organisms	<i>Pseudomonas</i>	0.43	1.36	15.79	[39]
	<i>Thauera</i>	0	0.02	7.01	[40]
	<i>Acinetobacter</i>	12.47	0.32	3.21	[41]
	<i>Gemmatimonas</i>	0	2.39	0.01	[43]
	<i>Leptolyngbyales</i>	0.02	1.8	0.61	[14]

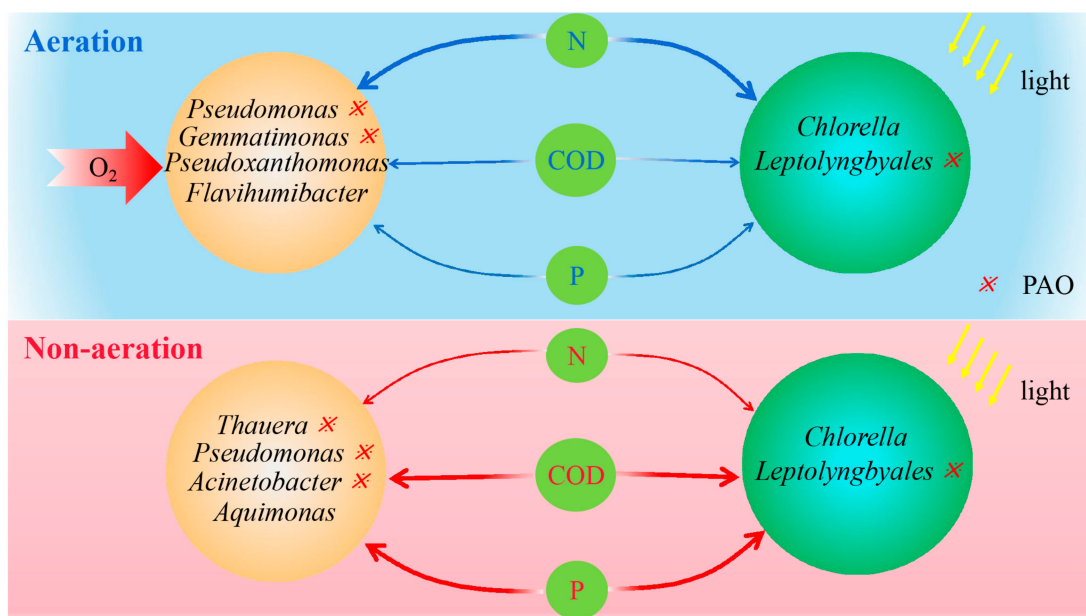


**Figure 4.** Possible pollutant removal pathways based on key functional microbial groups in the microalgal-bacterial granular sludge process under aeration and non-aeration conditions.

As shown in Figure 5, the reactor performance and microbial community evolution were investigated in the reactivation of long-term frozen stored MBGS under aeration and non-aeration conditions for the first time. Results showed that the frozen stored MBGS could fully recover activity after 21 days of activation, which provided important information that can be applied when the MBGS was faced with sludge storage and transport problems during practical applications. These two different methods had their different characteristics, as illustrated in Figure 5. The aeration favored biomass growth, especially in the growth of eukaryotic microalgae, Chl content, and ammonia removal. Contrarily, the non-aeration method favored particle size, EPS secretion, prokaryotic microalgae growth, and organics and phosphorus removal. Considering the environmental and economic sustainability in waste treatment [44], the non-aeration conditions were more promising in frozen MBGS recovery than the aeration conditions.

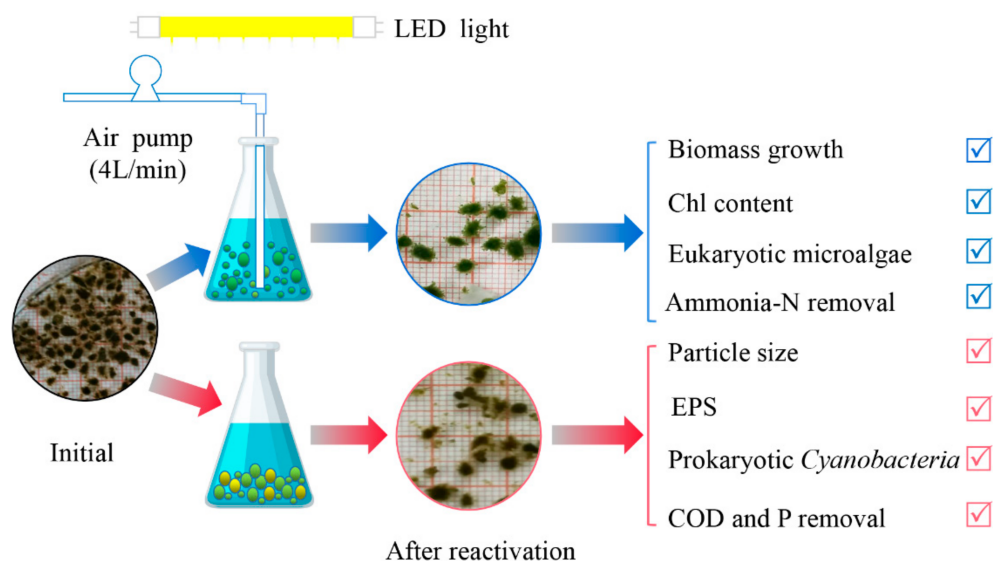


**Figure 5.** Overall characteristics of reactivation of frozen stored microalgal-bacterial granular sludge under aeration and non-aeration conditions.

#### 4. Conclusions

This paper presented the first study on the reactivation of frozen stored MBGS in aeration and non-aeration conditions. It proved that granular structure and activity could be fully restored after 21 days of reactivation. The recovered system under aeration conditions was efficient in ammonia removal. Meanwhile, the recovered system without aeration favored the removal of organics and phosphorus. In addition, microbial communities were also subverted, with *Chlorophyta* and *Proteobacteria* being the dominant species. Overall, the reactivation of MBGS without aeration seemed to be more energy-saving and promising.

**Supplementary Materials:** The following are available online at <https://www.mdpi.com/article/10.3390/w13141974/s1>, Figure S1: Variation in morphological appearances of microalgal-bacterial granules (a) Aerated PBR; (b) Non-aerated PBR during the reactivation process, Figure S2: Microbial community reflected by microscope and SEM of microalgal-bacterial granules. Aerated PBR: (a) microscope; (b) SEM. Non-aerated PBR: (c) microscope; (d) SEM, Figure S3: Particle size distributions of microalgal-bacterial granules after reactivation. (R1: Aeration; R2: Non-aeration).

**Author Contributions:** Conceptualization, B.J.; methodology, B.J. and L.Z.; validation, Y.M.; investigation, L.Z. and Y.X.; data curation, L.Z. and Y.S.; writing—original draft preparation, Y.S.; writing—review and editing, B.J., Y.M. and S.F.; All authors have read and agreed to the published version of the manuscript.

**Funding:** This research received no external funding.

**Institutional Review Board Statement:** Not applicable.

**Informed Consent Statement:** Informed consent was obtained from all subjects involved in the study.

**Data Availability Statement:** Not applicable.

**Conflicts of Interest:** The authors declare no conflict of interest.

#### References

- Zhang, X.; Zhang, M.; Liu, H.; Gu, J.; Liu, Y. Environmental sustainability: A pressing challenge to biological sewage treatment processes. *Curr. Opin. Environ. Sci. Health* **2019**, *12*, 1–5. [[CrossRef](#)]
- Nordlander, E.; Olsson, J.; Thorin, E.; Nehrenheim, E. Simulation of energy balance and carbon dioxide emission for microalgae introduction in wastewater treatment plants. *Algal Res.* **2017**, *24*, 251–260. [[CrossRef](#)]

3. Guo, W.-Q.; Yang, S.-S.; Xiang, W.-S.; Wang, X.-J.; Ren, N.-Q. Minimization of excess sludge production by in-situ activated sludge treatment processes—A comprehensive review. *Biotechnol. Adv.* **2013**, *31*, 1386–1396. [[CrossRef](#)]
4. Franca, R.D.; Pinheiro, H.M.; van Loosdrecht, M.C.; Lourenço, N.D. Stability of aerobic granules during long-term bioreactor operation. *Biotechnol. Adv.* **2018**, *36*, 228–246. [[CrossRef](#)]
5. Ji, B.; Zhang, M.; Gu, J.; Ma, Y.; Liu, Y. A self-sustaining synergetic microalgal-bacterial granular sludge process towards energy-efficient and environmentally sustainable municipal wastewater treatment. *Water Res.* **2020**, *179*, 115884. [[CrossRef](#)]
6. Zhang, M.; Ji, B.; Liu, Y. Microalgal-bacterial granular sludge process: A game changer of future municipal wastewater treatment? *Sci. Total Environ.* **2021**, *752*, 141957. [[CrossRef](#)]
7. Huang, W.; Liu, D.; Huang, W.; Cai, W.; Zhang, Z.; Lei, Z. Achieving partial nitrification and high lipid production in an algal-bacterial granule system when treating low COD/NH<sub>4</sub>-N wastewater. *Chemosphere* **2020**, *248*, 126106. [[CrossRef](#)]
8. Wang, J.; Lei, Z.; Wei, Y.; Wang, Q.; Tian, C.; Shimizu, K.; Zhang, Z.; Adachi, Y.; Lee, D. Behavior of algal-bacterial granular sludge in a novel closed photo-sequencing batch reactor under no external O<sub>2</sub> supply. *Bioresour. Technol.* **2020**, *318*, 124190. [[CrossRef](#)]
9. Wang, S.; Ji, B.; Cui, B.; Ma, Y.; Guo, D.; Liu, Y. Cadmium-effect on performance and symbiotic relationship of microalgal-bacterial granules. *J. Clean. Prod.* **2021**, *282*, 125383. [[CrossRef](#)]
10. Wang, S.; Ji, B.; Zhang, M.; Ma, Y.; Gu, J.; Liu, Y. Defensive responses of microalgal-bacterial granules to tetracycline in municipal wastewater treatment. *Bioresour. Technol.* **2020**, *312*, 123605. [[CrossRef](#)]
11. Huang, W.; Li, B.; Zhang, C.; Zhang, Z.; Lei, Z. Effect of algae growth on aerobic granulation and nutrients removal from synthetic wastewater by using sequencing batch reactors. *Bioresour. Technol.* **2015**, *179*, 187–192. [[CrossRef](#)]
12. Zhao, Z.; Yang, X.; Cai, W.; Lei, Z.; Shimizu, K.; Zhang, Z.; Utsumi, M.; Lee, D. Response of algal-bacterial granular system to low carbon wastewater: Focus on granular stability, nutrients removal and accumulation. *Bioresour. Technol.* **2018**, *268*, 221–229. [[CrossRef](#)]
13. Meng, F.; Liu, D.; Huang, W.; Lei, Z.; Zhang, Z. Effect of salinity on granulation, performance and lipid accumulation of algal-bacterial granular sludge. *Bioresour. Technol. Rep.* **2019**, *7*, 100228. [[CrossRef](#)]
14. Ji, B.; Zhang, M.; Wang, L.; Wang, S.; Liu, Y. Removal mechanisms of phosphorus in non-aerated microalgal-bacterial granular sludge process. *Bioresour. Technol.* **2020**, *312*, 123531. [[CrossRef](#)] [[PubMed](#)]
15. Liu, Y.; Gu, J.; Zhang, M. *AB Processes: Towards Energy Self-Sufficient Municipal Wastewater Treatment*; IWA Publishing: London, UK, 2019.
16. Ji, B.; Yang, K.; Zhu, L.; Jiang, Y.; Wang, H.; Zhou, J.; Zhang, H. Aerobic denitrification: A review of important advances of the last 30 years. *Biotechnol. Bioprocess Eng.* **2015**, *20*, 643–651. [[CrossRef](#)]
17. Ji, B.; Zhu, L.; Wang, S.; Liu, Y. Temperature-effect on the performance of non-aerated microalgal-bacterial granular sludge process in municipal wastewater treatment. *J. Environ. Manag.* **2021**, *282*, 111955. [[CrossRef](#)]
18. Zhang, B.; Guo, Y.; Lens, P.N.L.; Zhang, Z.; Shi, W.; Cui, F.; Tay, J.H. Effect of light intensity on the characteristics of algal-bacterial granular sludge and the role of N-acyl-homoserine lactone in the granulation. *Sci. Total Environ.* **2019**, *659*, 372–383. [[CrossRef](#)]
19. Lv, Y.; Wan, C.; Liu, X.; Zhang, Y.; Lee, D.; Tay, J. Freezing of aerobic granules for storage and subsequent recovery. *J. Taiwan Inst. Chem. Eng.* **2013**, *44*, 770–773. [[CrossRef](#)]
20. Gao, D.; Yuan, X.; Liang, H. Reactivation performance of aerobic granules under different storage strategies. *Water Res.* **2012**, *46*, 3315–3322. [[PubMed](#)]
21. Ji, B.; Zhu, L.; Wang, S.; Qin, H.; Ma, Y.; Liu, Y. A novel micro-ferrous dosing strategy for enhancing biological phosphorus removal from municipal wastewater. *Sci. Total Environ.* **2020**, *704*, 135453. [[CrossRef](#)] [[PubMed](#)]
22. Zhang, B.; Lens, P.N.L.; Shi, W.; Zhang, R.; Zhang, Z.; Guo, Y.; Bao, X.; Cui, F. Enhancement of aerobic granulation and nutrient removal by an algal-bacterial consortium in a lab-scale photobioreactor. *Chem. Eng. J.* **2018**, *334*, 2373–2382. [[CrossRef](#)]
23. Federation, Water Environmental, and APH Association. *Standard Methods for the Examination of Water and Wastewater*, 21th ed.; American Public Health Association: Washington, DC, USA, 2005.
24. He, Q.; Chen, L.; Zhang, S.; Chen, R.; Wang, H.; Zhang, W.; Song, J. Natural sunlight induced rapid formation of water-born algal-bacterial granules in an aerobic bacterial granular photo-sequencing batch reactor. *J. Hazard. Mater.* **2018**, *359*, 222–230. [[CrossRef](#)]
25. Lee, C.S.; Lee, S.; Ko, S.; Oh, H.; Ahn, C. Effects of photoperiod on nutrient removal, biomass production, and algal-bacterial population dynamics in lab-scale photobioreactors treating municipal wastewater. *Water Res.* **2015**, *68*, 680–691. [[CrossRef](#)] [[PubMed](#)]
26. Tang, T.; Fadaei, H.; Hu, Z. Rapid evaluation of algal and cyanobacterial activities through specific oxygen production rate measurement. *Ecol. Eng.* **2014**, *73*, 439–445. [[CrossRef](#)]
27. Sayara, T.; Khayat, S.; Saleh, J.; Abu-Khalaf, N.; van der Steen, P. Algal-bacterial symbiosis for nutrients removal from wastewater: The application of multivariate data analysis for process monitoring and control. *Environ. Technol. Innov.* **2021**, *23*, 101548. [[CrossRef](#)]
28. Yang, J.; Li, Z.; Lu, L.; Fang, F.; Guo, J.; Ma, H. Model-based evaluation of algal-bacterial systems for sewage treatment. *J. Water Process Eng.* **2020**, *38*, 101568. [[CrossRef](#)]
29. Boelee, N.C.; Temmink, H.; Janssen, M.; Buisman, C.J.N.; Wijffels, R.H. Balancing the organic load and light supply in symbiotic microalgal-bacterial biofilm reactors treating synthetic municipal wastewater. *Ecol. Eng.* **2014**, *64*, 213–221. [[CrossRef](#)]

30. Abouhend, A.S.; Milferstedt, K.; Hamelin, J.; Ansari, A.A.; Butler, C.; Carbajal-González, B.I.; Park, C. Growth progression of oxygenic photogranules and its impact on bioactivity for aeration-free wastewater treatment. *Environ. Sci. Technol.* **2019**, *54*, 486–496. [[CrossRef](#)]
31. Liu, L.; Fan, H.; Liu, Y.; Liu, C.; Huang, X. Development of algae-bacteria granular consortia in photo-sequencing batch reactor. *Bioresour. Technol.* **2017**, *232*, 64–71. [[CrossRef](#)]
32. He, Q.; Zhang, W.; Zhang, S.; Zou, Z.; Wang, H. Performance and microbial population dynamics during stable operation and reactivation after extended idle conditions in an aerobic granular sequencing batch reactor. *Bioresour. Technol.* **2017**, *238*, 116–121. [[CrossRef](#)]
33. Arcila, J.S.; Buitrón, G. Influence of solar irradiance levels on the formation of microalgae-bacteria aggregates for municipal wastewater treatment. *Algal Res.* **2017**, *27*, 190–197. [[CrossRef](#)]
34. Zhang, L.; Long, B.; Wu, J.; Cheng, Y.; Zhang, B.; Zeng, Y.; Huang, S.; Zeng, M. Evolution of microbial community during dry storage and recovery of aerobic granular sludge. *Heliyon* **2019**, *5*, e3023. [[CrossRef](#)]
35. Wan, C.; Zhang, Q.; Lee, D.; Wang, Y.; Li, J. Long-term storage of aerobic granules in liquid media: Viable but non-culturable status. *Bioresour. Technol.* **2014**, *166*, 464–470. [[CrossRef](#)] [[PubMed](#)]
36. Cheng, R.; Zhu, H.; Shutes, B.; Yan, B. Treatment of microcystin (MC-LR) and nutrients in eutrophic water by constructed wetlands: Performance and microbial community. *Chemosphere* **2021**, *263*, 128139. [[CrossRef](#)] [[PubMed](#)]
37. Szabó, E.; Liébana, R.; Hermansson, M.; Modin, O.; Persson, F.; Wilén, B. Microbial Population Dynamics and Ecosystem Functions of Anoxic/Aerobic Granular Sludge in Sequencing Batch Reactors Operated at Different Organic Loading Rates. *Front. Microbiol.* **2017**, *8*. [[CrossRef](#)]
38. Meng, F.; Xi, L.; Liu, D.; Huang, W.; Lei, Z.; Zhang, Z.; Huang, W. Effects of light intensity on oxygen distribution, lipid production and biological community of algal-bacterial granules in photo-sequencing batch reactors. *Bioresour. Technol.* **2019**, *272*, 473–481. [[CrossRef](#)]
39. Wang, H.; Zhang, W.; Ye, Y.; He, Q.; Zhang, S. Isolation and Characterization of *Pseudoxanthomonas* sp. Strain YP1 Capable of Denitrifying Phosphorus Removal (DPR). *Geomicrobiol. J.* **2018**, *35*, 537–543. [[CrossRef](#)]
40. Wang, Q.; He, J. Complete nitrogen removal via simultaneous nitrification and denitrification by a novel phosphate accumulating *Thauera* sp. strain SND5. *Water Res.* **2020**, *185*, 116300. [[CrossRef](#)] [[PubMed](#)]
41. Izadi, P.; Izadi, P.; Eldyasti, A. Enhancement of simultaneous nitrogen and phosphorus removal using intermittent aeration mechanism. *J. Environ. Sci.* **2021**, *109*, 1–14. [[CrossRef](#)]
42. Ren, T.T.; Jin, C.Z.; Jin, F.J.; Li, T.; Kim, C.J.; Oh, H.M.; Lee, H.G.; Jin, L. *Flaviumibacter profundus* sp. nov., isolated from eutrophic freshwater sediment. *J. Microbiol.* **2018**, *56*, 467–471. [[CrossRef](#)] [[PubMed](#)]
43. Zhang, H.; Sekiguchi, Y.; Hanada, S.; Hugenholtz, P.; Kim, H.; Kamagata, Y.; Nakamura, K. *Gemmatimonas aurantiaca* gen. nov., sp. nov., a gram-negative, aerobic, polyphosphate-accumulating micro-organism, the first cultured representative of the new bacterial phylum Gemmatimonadetes phyl. nov. *Int. J. Syst. Evol. Microbiol.* **2003**, *53*, 1155–1163. [[CrossRef](#)] [[PubMed](#)]
44. Ma, Y.; Liu, Y. Turning food waste to energy and resources towards a great environmental and economic sustainability: An innovative integrated biological approach. *Biotechnol. Adv.* **2019**, *37*, 107414. [[CrossRef](#)] [[PubMed](#)]